Journal of Organometallic Chemistry 768 (2014) 28–35

Contents lists available at ScienceDirect

Journal of Organometallic Chemistry

journal homepage: www.elsevier.com/locate/jorganchem

New electropolymerizable metal-free, metallophthalocyanines and their electrochemical, spectroelectrochemical studies

Volkan Çakır [a], Halit Kantekin [a, *], Zekeriya Bıyıklıoğlu [a], Atıf Koca [b]

[a] Department of Chemistry, Faculty of Science, Karadeniz Technical University, 61080 Trabzon, Turkey
[b] Department of Chemical Engineering, Engineering Faculty, Marmara University, Göztepe, 34722 İstanbul, Turkey

ARTICLE INFO

Article history:
Received 12 February 2014
Received in revised form
4 June 2014
Accepted 12 June 2014
Available online 21 June 2014

Keywords:
Phthalocyanine
Cobalt
Synthesis
Electropolymerization
Electrochemistry
Spectroelectrochemistry

ABSTRACT

The synthesis, characterization of newly synthesized metal-free **4** and metallophthalocyanine complexes **5**–**7** (MPcs, M = Ni, Co, Cu) have been presented in this work. All the new phthalocyanine compounds are characterized by a combination of IR, ^{1}H and ^{13}C NMR, mass and UV–Vis spectroscopy techniques. Voltammetric and spectroelectrochemical analyses of phthalocyanines supported the proposed structure of the synthesized complexes. All complexes were oxidatively electropolymerized on the working electrode during the repetitive anodic potential scans. Formation of thin film of the complex as a result of electropolymerization, and controlling the film characters by altering the excitation signals of the voltammetry, changing the working electrode and metal center of the complexes affects the polymerization mechanisms.

Introduction

Metal-free and metallophthalocyanines are very important compounds because they have been used in very different areas of technology and medical applications for example photodynamic therapy of cancer [1,2], chemical sensors [3], photoconductors [4], electrochromic display [5], catalysis [6–9], liquid crystal [10] and nanotechnology [11,12]. Despite many inherent chemical advantages of phthalocyanine complexes their one of the most important disadvantage is insolubility in common organic solvents. Substituents can bound on phthalocyanine ring its periferal or non-periferal positions and depending on the polarity of the substituents, substituted phthalocyanines become more soluble in apolar or polar solvents [13–18].

Metallophthalocyanines exhibit interesting electrochemical and spectroelectrochemical properties just because their properties may be remarkably affected by the chemical character of central metal ions and the nature of (electron-withdrawing or electron-donating) and position (peripheral or non peripheral) of substituent on the phthalocyanine ring [19–22]. Spectroelectrochemical studies of metallophthalocyanines are also important with regard to their possible usage as electrochromic materials, where several colors are displayed based on the potential applied to the electrode surface [23–25]. Therefore, in this paper we have investigated electrochemical and spectroelectrochemical properties of these newly synthesized complexes. We have also aimed to prepare modified electrodes with electropolymerization of the complexes.

Experimental

Materials

2-{2-[3-(Diethylamino)phenoxy]ethoxy}ethanol **1** [26], 4-nitrophthalonitrile **2** [27], 4-(2-{2-[3-(diethylamino)phenoxy]ethoxy}ethoxy)phthalonitrile **3** [28] were prepared according to the literature procedure. All reagents and solvents were of reagent grade quality and were obtained from commercial suppliers. All solvents were dried and purified as described by Perrin and Armarego [29].

Equipment

The IR spectra were recorded on a Perkin Elmer 1600 FT-IR spectrophotometer, using KBr pellets. ^{1}H and ^{13}C NMR spectra were recorded on a Varian Mercury 300 MHz spectrometer in $CDCl_3$, and chemical shifts were reported (δ) relative to Me_4Si as internal standard. Mass spectra were measured on a Micromass

* Corresponding author. Tel.: +90 462 377 25 89; fax: +90 462 325 31 96.
E-mail address: halit@ktu.edu.tr (H. Kantekin).

http://dx.doi.org/10.1016/j.jorganchem.2014.06.006
0022-328X/

Quatro LC/ULTIMA LC–MS/MS spectrometer. MALDI–MS of complexes were obtained in dihydroxybenzoic acid as MALDI matrix using nitrogen laser accumulating 50 laser shots using Bruker Microflex LT MALDI–TOF mass spectrometer. Optical spectra in the UV–Vis region were recorded with a Perkin Elmer Lambda 25 spectrophotometer. Melting points were measured on an electrothermal apparatus and are uncorrected.

Electrochemical and spectroelectrochemical measurements

Cyclic voltammetry (CV) and square wave voltammetry (SWV) measurements were carried out with Gamry Reference 600 potentiostat/galvanostat. The working electrode was a Pt disc with a surface area of 0.071 cm^2. A Pt wire served as the counter electrode. Saturated calomel electrode (SCE) was employed as the reference electrode. Electrochemical grade tetrabuthylammonium perchlorate (TBAP) in extra pure dichloromethane (DCM) or dimethyl sulfoxide (DMSO) was employed as the supporting electrolyte.

An OceanOptics QE65000 diode array spectrophotometer was used for UV–Vis absorption spectra and chromaticity diagram measurements. *In-situ* spectroelectrochemical measurements were carried out by utilizing a three-electrode configuration of thin-layer quartz thin-layer spectroelectrochemical cell consisting a Pt tulle working electrode, a Pt wire counter electrode, and an SCE reference electrode.

Synthesis

*Synthesis of metal-free phthalocyanine (**4**)*

A mixture of 4-(2-{2-[3-(Diethylamino)phenoxy]ethoxy} ethoxy)phthalonitrile (**3**) (0.350 g, 9,2 × 10^{-4} mol), 4 drops of 1.8-diazabicyclo[5.4.0]undec-7-ene (DBU) in n-pentanol (3.5 × 10^{-3} L) was heated to 160 °C with stirring for 24 h under N_2 gas atmosphere. After the reaction mixture was cooled at room temperature and precipitated by adding ethanol. The crude solid product was filtered and washed with ethanol, water and diethyl ether. Finally, pure metal-free phthalocyanine was obtained by column chromatography which is placed aluminium oxide using $CHCl_3$:CH_3OH (100:1) as solvent system.Yield: 0.079 g (23%). IR (KBr tablet) ν_{max}/cm^{-1}: 3291 (N–H), 3072 (Ar–H), 2967–2869 (Aliph. C–H), 1603, 1569, 1497, 1469, 1394, 1373, 1344, 1323, 1274, 1211, 1129, 1092, 1009, 819, 745, 716, 686. ^{1}H NMR. ($CDCl_3$), (δ:ppm): 8.28-8.26 (m, 4H, Ar–H), 7.42-7.24 (m, 12H, Ar–H), 6.74-6.64 (m, 4H, Ar–H), 6.36-6.35 (s, 8H, Ar–H), 4.32-4.14 (m, 32H, CH_2–O), 3.47-3.32 (m, 16H, CH_2–N), 1.15 (s, 24H, CH_3). ^{13}C NMR. ($CDCl_3$), (δ:ppm): 165.99, 149.94, 149.46, 138.22, 131.42, 130.85, 130.25, 130.21, 109.99, 105.59, 105.55, 101.09, 101.04, 99.45, 70.52, 67.53, 44.62, 12.90. UV–Vis (chloroform): λ_{max}, nm (log ε): 342 (4.84), 387 (4.55), 607 (4.46), 641 (4.64), 669 (5.00), 704 (5.06). MALDI–TOF–MS *m*/*z*: 1520 $[M+H]^+$.

*General procedures for metallophthalocyanine derivatives (**5**–**7**)*

A mixture of **3** (0.350 g, 9,2 × 10^{-4} mol), n-pentanol (4 × 10^{-3} L), anhydrous metal salt (4,6 × 10^{-4} mol; 0.061 g $NiCl_2$, 0.060 g $CoCl_2$, 0.062 g $CuCl_2$) and 1.8-diazabicyclo[5.4.0]undec-7-ene (DBU) (5 drops) was refluxed under N_2 for 24 h. After cooling to room temperature, ethanol was added in order to precipitate the product. The green product was filtered off and washed ethanol, water and diethyl ether. Finally, pure metallophthalocyanines were obtained by column chromatography which is placed aluminium oxide using $CHCl_3$:CH_3OH (100:1) as solvent system.

*Nickel(II) phthalocyanine (**5**)*

Yield: 0.100 g (27%). IR (KBr tablet) ν_{max}/cm^{-1}: 3070 (Ar–H), 2966-2869 (Aliph. C–H), 1603, 1569, 1532, 1497, 1467, 1411, 1373, 1351, 1272, 1215, 1120, 1090, 1063, 1021, 988, 964, 819, 783, 749, 686. ^{1}H NMR. ($CDCl_3$), (δ:ppm): 7.87-7.69 (m, 4H, Ar–H), 7.36-7.18 (m, 12H, Ar–H), 6.72-6.62 (m, 4H, Ar–H), 6.36-6.35 (s, 8H, Ar–H), 4.29-4.13 (m, 32H, CH_2–O), 3.45-3.33 (m, 16H, CH_2–N), 1.16 (s, 24H, CH_3). ^{13}C NMR. ($CDCl_3$), (δ:ppm): 160.56, 149.81, 149.46, 132.97, 131.13, 130.74, 130.23, 130.17, 105.53, 105.51, 105.48, 101.11, 101.07, 99.48, 70.43, 67.42, 44.64, 12.93. UV–Vis (chloroform): λ_{max}, nm (log ε): 326 (4.79), 380 (4.54), 608 (4.54), 675 (5.07). MALDI–TOF–MS *m*/*z*: 1576 $[M]^+$.

*Cobalt(II) phthalocyanine (**6**)*

Yield: 0.085 g (23%). IR (KBr tablet) ν_{max}/cm^{-1}: 3067 (Ar–H), 2967-2872 (Aliph. C–H), 1604, 1589, 1498, 1464, 1374, 1355, 1273, 1216, 1122, 1092, 1063, 1022, 988, 965, 819, 751, 686. UV–Vis (chloroform): λ_{max}, nm (log ε): 376 (4.70), 611 (4.59), 674 (5.01). MS (ESI), (*m*/*z*): 1598 $[M+Na]^+$

*Copper(II) phthalocyanine (**7**)*

Yield: 0.100 g (27%). IR (KBr tablet) ν_{max}/cm^{-1}: 3074 (Ar–H), 2966-2869 (Aliph. C–H), 1603, 1569, 1467, 1396, 1374, 1342, 1273, 1216, 1118, 1090, 1057, 1021, 988, 960, 819, 783, 745, 685. UV–Vis (chloroform): λ_{max}, nm (log ε): 338 (4.77), 380 (4.40), 615 (4.53), 683 (5.04). MALDI–TOF–MS *m*/*z*: 1581 $[M]^+$.

Results and discussion

Synthesis and characterization

The general synthetic route of new metal-free and metallophthalocyanines (**5**–**7**) is given in Fig. 1. The metal-free phthalocyanine **4** was accomplished in n-pentanol in the presence of a few drops of 1,8-diazabicyclo[5.4.0]undec-7-ene (DBU) as a strong base at reflux temperature under N_2 gas atmosphere. The novel nickel(II), cobalt(II) and copper(II) phthalocyanines (**5**–**7**) were prepared by the templated cyclotetramerization reaction from 4-(2-{2-[3-(diethylamino)phenoxy]ethoxy}ethoxy)phthalonitrile **3** and metal salts ($NiCl_2$, $CoCl_2$, $CuCl_2$) in n-pentanol and DBU at 160 °C. Metal-free and metallophthalocyanines were purified by column chromatography. The structures of the target compounds were confirmed using UV–Vis, IR, ^{1}H NMR, ^{13}C NMR, MS spectroscopic data. The analyses are consistent with the predicted structures as shown in the experimental section.

In the IR spectrum of metal-free phthalocyanine (**4**), the peak at 3291 cm^{-1} is characteristic peak for the metal-free phthalocyanine N–H stretching vibration band (see the "Supplementary Information" file). The ^{1}H NMR spectra of compound (**4**) was in agreement with the proposed structure. The ^{1}H NMR spectra of metal-free phthalocyanine (**4**) showed aromatic protons between 8.28 and 6.35 ppm with the aliphatic protons observed between 4.32 and 1.15 ppm for the complex (see the "Supplementary Information" file). The NH protons of compound **4** could not be observed owing to the probable strong aggregation of the molecules [30]. The ^{13}C NMR spectra of the compound **4** indicated 18 carbon atoms between at 165.99–12.90 ppm. In general, phthalocyanines show typical electronic spectra with two strong absorption regions, one in the UV region at about 300–500 nm related to the B band and the other in the visible region at 600–700 nm related to the Q band. UV–Vis spectrum of metal-free phthalocyanine (**4**) in chloroform, the characteristic split Q bands were observed with absorptions at 704 and 669 nm which can be attributed $a_{1u} \rightarrow e_g$ transition [31]. UV–Vis spectrum of the metal-free phthalocyanine (**4**) in chloroform showed a B band region at

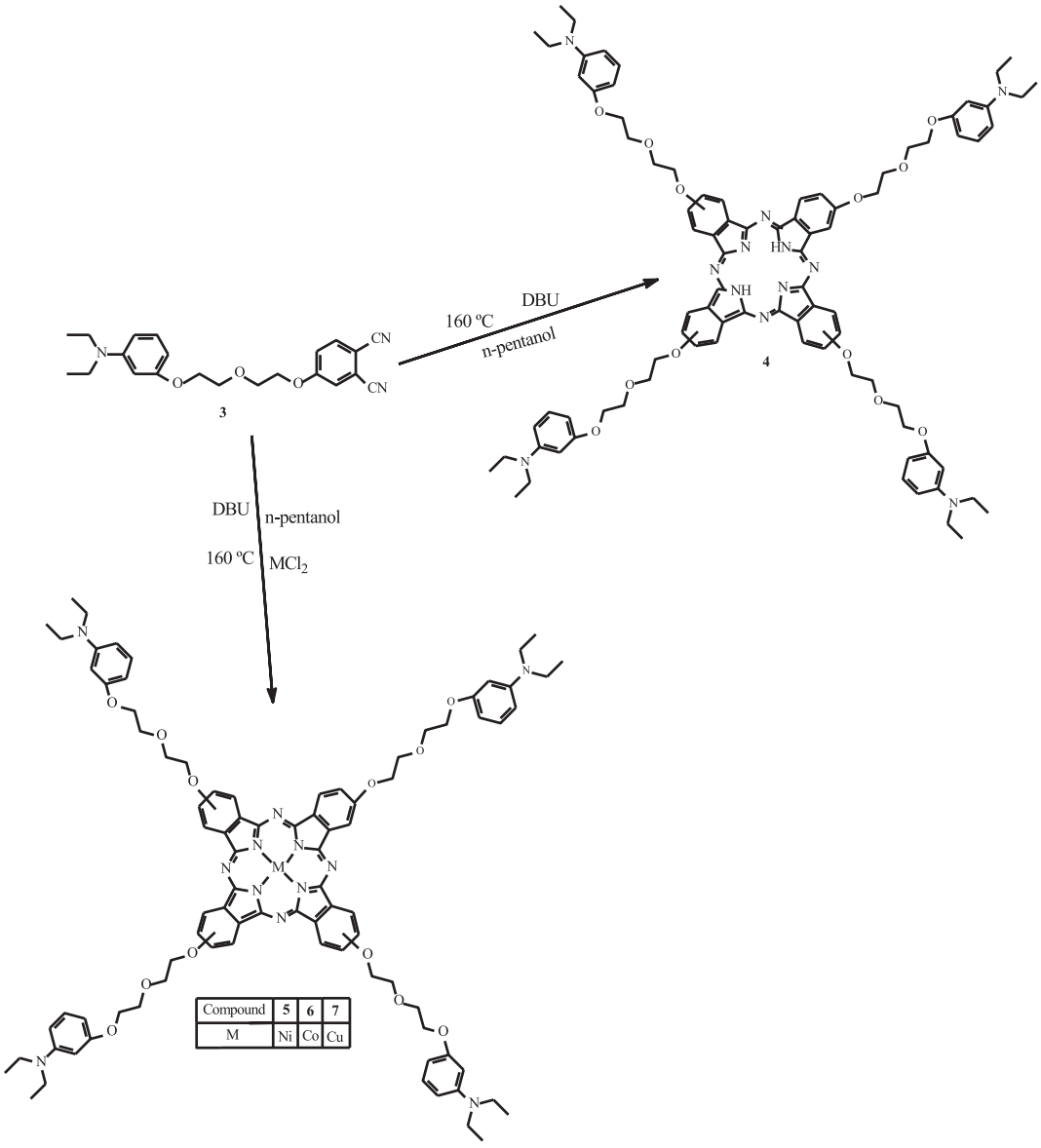

Fig. 1. The synthetic route of the metal-free (**4**) and metallophthalocyanines (**5**–**7**). MCl_2: $NiCl_2$, $CoCl_2$, $CuCl_2$.

387 and 342 nm. MALDI–TOF mass spectrum of compound (**4**) shows a peak at $m/z = 1520$ $[M+H]^+$.

The IR spectrum of nickel(II), cobalt(II) and copper(II) phthalocyanines **5**–**7** clearly indicated the cyclotetramerization of the phthalonitrile derivative **3** with the disappearance of the C≡N peak at 2233 cm^{-1} (see the "Supplementary Information" file). Characteristic metal free phthalocyanine N–H stretching bands (at 3291 cm^{-1}) is especially beneficial for the characterization of metal-free phthalocyanine (**4**), this band disappeared in the IR spectra of the metallophthalocyanine derivatives (**5**–**7**). The ^1H NMR spectrum of nickel(II) phthalocyanine **5** indicated the aromatic protons at 7.87–6.35 ppm and aliphatic protons at 4.29–1.16 ppm (see the "Supplementary Information" file). ^1H NMR measurement of the cobalt(II) and copper(II) phthalocyanine (**6**), (**7**) was precluded owing to its paramagnetic nature [32]. The electronic absorption spectra of the metal-free and metallophthalocyanines (**4**), (**5**), (**6**) and (**7**), in chloroform at room temperature are shown in Fig. 2. The Q band absorptions in the UV–Vis absorption spectra of the metallophthalocyanines (**5**, **6** and **7**) were observed as single Q bands with high intensity due to a single $\pi-\pi^*$ transition at 675, 674 and 683 nm, respectively. B bands of the metallophthalocyanines (**5**, **6** and **7**) were observed in the UV region at 326, 376 and 338 nm, respectively. These results were typical for metallophthalocyanine complexes. In the mass spectra of compounds (**5**–**7**), the parent molecular ion peaks were exhibited at $m/z = 1576$ $[M]^+$ for (**5**), 1598 $[M+Na]^+$ for (**6**) and 1581 $[M]^+$ for (**7**), these peaks have verified the proposed structures (see the "Supplementary Information" file).

Electrochemical measurements

Determination of the electrochemical behaviors of the MPc complexes is essential for to decide possible utility of the complexes in various electrochemical application fields. Therefore electrochemical properties of the complexes were determined in solution with CV and SWV techniques. Voltammetric responses of the complexes were analyzed and derived parameters were tabulated on Table 1. Basic electrochemical responses of the complexes

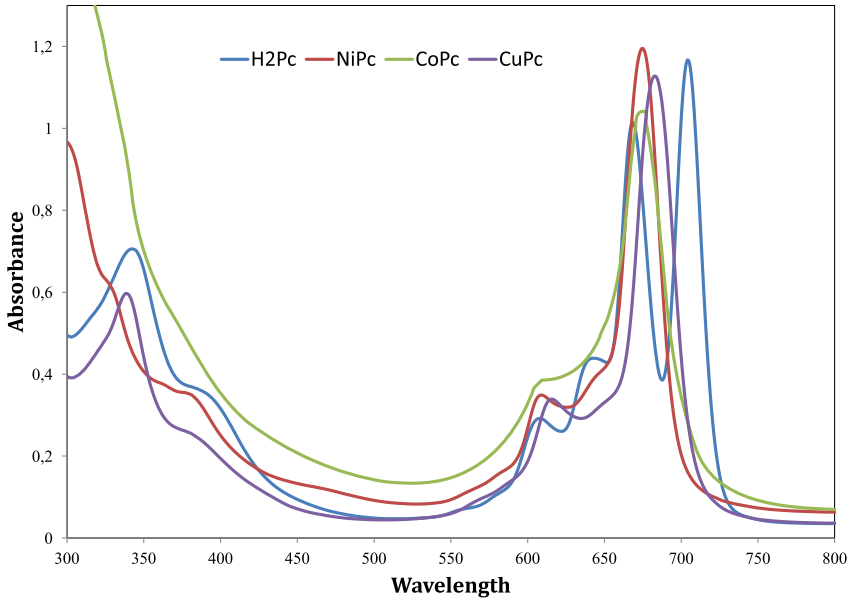

Fig. 2. UV–Vis spectrum of **4**, **5**, **6** and **7** in chloroform.

are in agreements with the similar complexes in the literature [33–35]. Effects of the metal ions in the Pc cores of the complexes to the redox features are well reflected with the overlay CVs of them (Fig. 3). As shown in this figure, **H_2Pc**, **CuPc** and **NiPc** give two reversible reduction processes and these reduction reactions shift to the negative potentials with respect to the decreasing effective nuclear charge of the central metal ions. The most easily reduced one is **H_2Pc** and the most difficultly reduced one is **NiPc**. As shown in Fig. 3, redox properties of **CoPc** are completely different than others. While **H_2Pc**, **CuPc** and **NiPc** give two reversible reduction processes between −0.70 and −1.20 V, **CoPc** give the first reduction process at a more smaller potential (−0.70 V) and second reduction peak at a far potential (−1.20 V) than the others. This uncommon redox behavior of **CoPc** is resulted from the redox activity of Co^{II} metal ion of the complex. Due to the existence of the empty "d" orbital of Co^{II} metal ion between the energy level of the highest occupied molecular orbital (HOMO) and the lowest unoccupied molecular orbital (LUMO) of Pc ring, Co^{II} can reduce before Pc ring, the R_1 process of **CoPc** is observed at −0.28 V and easily assigned to the Co^{II}/Co^{I} reduction reaction of the complex. Among the complexes, **CoPc** is the most valuable one due to the redox activity of the metal center of the complex. Since redox activity of the Co^{II} center of **CoPc** type complexes has made them functional materials in various electrochemical technologies, such as electrocatalytic [36,37] and electrosensing [38] applications.

Therefore electrochemical responses of **CoPc** were also analyzed with CVs recorded at different scan rates (Fig. 4). Scan rate analysis of CoPc indicates quasi-reversible peak character of the reduction reactions with respect to ΔE_p and I_{pa}/I_{pc} values of these redox couples. ΔE_p of R_1 and R_2 are 80 and 110 mV at 0.01 V s^{-1} respectively and this value increase up to 120 and 156 mV at 0.50 V s^{-1}. These analyses show electrochemical quasi-reversible character of these processes. Scan rate effects to I_{pa}/I_{pc} analyses of these redox couples indicate chemical irreversibility of R_1 couple. While I_{pa}/I_{pc} value is unity at slow scan rates, it gets 1.2 at 0.50 V s^{-1}. These data indicate existence of a chemical reaction to the electron transfer reaction. This chemical reaction is most probably aggregation disaggregation equilibrium of the complex. Under applied potentials, aggregation was diminished, thus reverse couple of the R1 process get bigger due to increasing monomer concentration. R'_1 wave observed at around −0.85 V could be easily assigned to the reduction of the aggregated CoPc species. Observation of this wave at faster scan rates supports aggregation assignments of the process. Aggregation property of the complex is also observed during spectroelectrochemical measurements (given below). Reversibility or irreversibility of these couples can be clearly shown in SWVs (Fig. 4(b)) [39]. CVs of **H_2Pc**, **CuPc** and **NiPc** complexes were recorded at different scan rates and given in the "Supplementary Information" file.

While **CoPc** gives metal based redox process in addition to the Pc based redox reactions, **H_2Pc**, **CuPc** and **NiPc** show only Pc based reduction reactions. All complexes studied electropolymerized during the anodic potential scans.

Fig. 5 illustrates CV responses of CoPc during repetitive CV cycles. During the first anodic scan, an anodic wave at 1.07 V and its reverse cathodic couple are recorded at 0.66 V. During the consecutive second CV cycle a new anodic wave is recorded at 0.75 V assigned to the polymerized complex. This new wave

Table 1
Voltammetric data of the complexes. All voltammetric data were given versus SCE.

Complex	Electropolymerization		M^{II}/M^{I}	Ring reductions	
CoPc	[a]$E_{1/2}$	1.07[d](0.66)[e]	−0.28 (−0.80)	−1.42	–
	[b]ΔE_p (mV)	–	80	110	–
	[c]$I_{p,a}/I_{p,c}$	–	1.03	0.86	–
H_2Pc	[a]$E_{1/2}$	1.12[d] (0.63)[e]	–	−0.70	−1.02
	[b]ΔE_p (mV)	–	–	160	175
	[c]$I_{p,a}/I_{p,c}$	–	–	0.94	0.93
CuPc	[a]$E_{1/2}$	1.01[d] (0.72)[e]	–	−0.85	−1.15
	[b]ΔE_p (mV)	–	–	150	120
	[c]$I_{p,a}/I_{p,c}$	–	–	0.96	0.91
NiPc	[a]$E_{1/2}$	1.00[d](0.72)[e]	–	−0.87	−1.19
	[b]ΔE_p (mV)	–	–	80	70
	[c]$I_{p,a}/I_{p,c}$	–	–	0.96	0.91

[a] $E_{1/2}$ values ($(E_{pa} + E_{pc})/2$) were given versus SCE at 0.100 V s^{-1} scan rate.
[b] $\Delta E_p = E_{pa} - E_{pc}$.
[c] $I_{p,a}/I_{p,c}$ for reduction, $I_{p,c}/I_{p,a}$ for oxidation processes.
[d] Anodic peak of the electropolymerization reaction recorded during first CV cycle.
[e] Cathodic peak of the electropolymerization reaction recorded during first CV cycle.

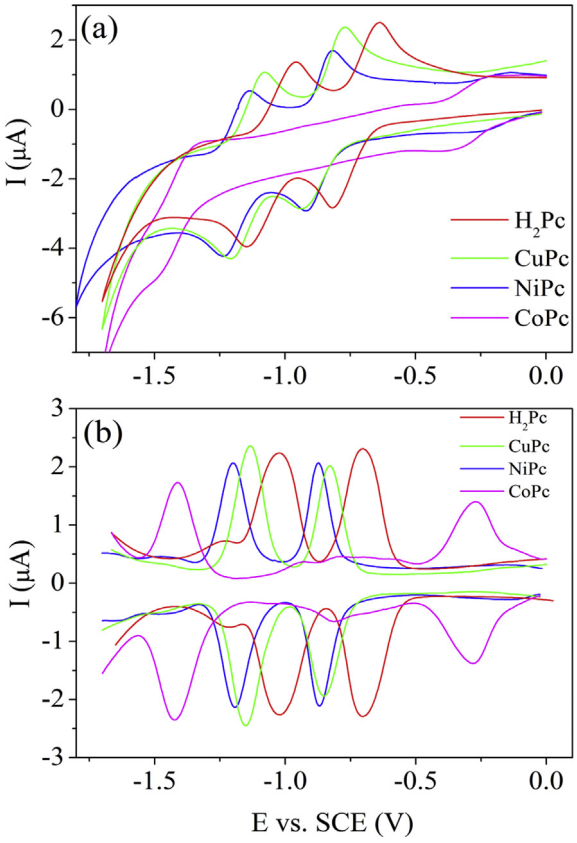

Fig. 3. (a) CVs of **4**, **5**, **6** and **7** (5.0 10^{-4} mol dm^{-3}) recorded at cathodic potentials at 0.100 V s^{-1} scan rate on a Pt working electrode in DCM/TBAP and (b) SWV of **4**, **5**, **6** and **7** recorded with SWV parameters: step size = 5 mV; pulse size = 100 mV; Frequency = 25 Hz.

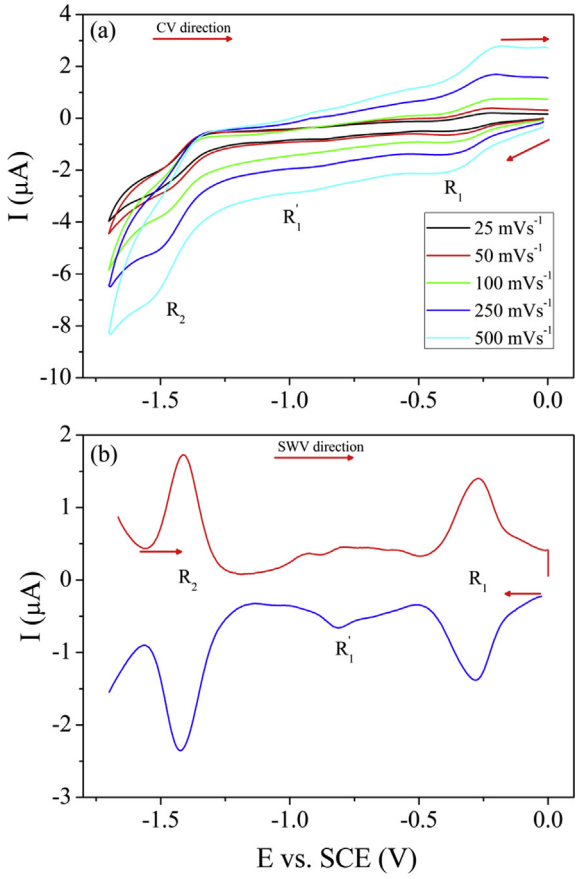

Fig. 4. (a) CV and SWV of **CoPc** (5.0 10^{-4} mol dm^{-3}) recorded at various scan rates on a Pt working electrode in DCM/TBAP (b) SWV of **CoPc**. (SWV parameters: step size = 5 mV; pulse size = 100 mV; Frequency = 25 Hz) (CV and SWV directions are shown with red arrows). (For interpretation of the references to color in this figure legend, the reader is referred to the web version of this article.)

increases in current intensity with a positive potential shift during 3 CV cycle. Then its peak current continuously decreases with a positive potential shift from 1.05 to 1.15 V until the 20 CV cycle. Similar CV responses were recorded for the cathodic wave. Moreover a new cathodic wave increases continuously at 0.32 V. These voltammetric responses of the complex illustrate coating of the complex on the working electrode with an electropolymerization process. The film on the electrode surface was seen easily with naked eyes. All complexes were electropolymerized on the working electrode with similar manners. But peak potentials or shifting trends of the peaks differed when metal centers were changed. CVs of the electropolymerization of **H_2Pc**, **CuPc** and **NiPc** complexes were given in the "Supplementary Information" file. Coating of the complexes on the working electrodes with electropolymerization processes indicated electrochemical application potentials of the complexes. Since electrode modification with electrtopolymerization is one of the most preferred modification techniques. Since it was possible to control all parameters of a modified electrode by controlling potential, concentration and or CV cycle numbers of the electropolymerization reactions [40–42]. Electropolymerization of the complexes are in harmony with our previous papers, in which we introduced electropolymerization of the complexes bearing {2,3-bis[3-(diethylamino)phenoxy]propoxy} groups [43] and octakis-[3-(diethylamino)phenoxy] [44] substituents. It was shown in these papers that amino group triggered the electropolymerization reaction of the complexes. It is shown that types of N-alkyl groups, length and type of the chain groups between Pc ring and amino nitrogen and metal center of MPc possible alter the polymerization properties of the complexes. Desired polymer of MPcs could be obtained by optimization of these relevant groups. Thus in this paper we used 2-{2-[3-(diethylamino)phenoxy] ethoxy}ethoxy substituted MPcs to illustrate effects of 2-{2-[3-(diethylamino)phenoxy]ethoxy}ethoxy moieties to the electropolymerization of MPcs.

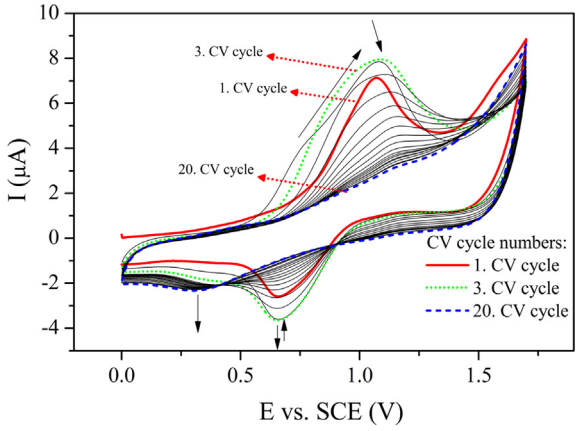

Fig. 5. Repetitive CVs of **CoPc** (5.0 10^{-4} mol dm^{-3}) recorded between 0.0 V and 1.70 V in DCM/TBAP electrolyte system at 0.100 V s^{-1} scan rate on a Pt working electrode. (CV directions are shown with red arrows and peak current changes are shown with black arrows. Red CV: 1. CV cycle; Green CV: 3. CV cycle; Blue CV: 20. CV cycle). (For interpretation of the references to color in this figure legend, the reader is referred to the web version of this article.)

Spectroelectrochemical studies

It is known that **H_2Pc**, **CuPc** and **NiPc** complexes give only Pc based electron transfer processes. Thus in situ spectroelectrochemical measurements during these redox process show Pc based spectral changes. In our previous papers we reported in situ spectroelectrochemical behaviors of many MPc complexes and spectral changes of **H_2Pc**, **CuPc** and **NiPc** are in harmony our previous papers [45–47]. During the reduction of MPcs, general trend of the spectral changes were decreasing the Q bands in intensity without shift and observation of new bands in the LMCT regions, which are characteristic changes for the MPcs having redox inactive metal centers. In situ UV–Vis spectral changes and in situ recorded chromaticity diagram of **CuPc** in DCM/TBAP during the electron transfer processes are given in Fig. 6 as a representative of MPcs having redox inactive metal centers. During the first reduction reaction, the Q band at 680 nm and its shoulder at 624 nm decrease in intensity and new bands at 578, 880 and 950 nm increase. These changes are easily assigned to $[Cu^{II}Pc^{-2}]$ to $[Cu^{II}Pc^{-3}]^{1-}$ (Fig. 6(a)) [45–47]. Clear isosbestic points are recorded at 595 and 795 nm during the first reduction reaction, which indicates production of one type of reduced species during the reduction reaction. A color changes from greenish blue ($x = 0.2433$ and $y = 0.3303$) to blue ($x = 0.2511$ and $y = 0.3064$) is recorded during the first reduction reaction (Fig. 6(d)). During the second reduction reaction the bands at 578, 624, 680 and 950 nm decreases, while the bands at 800 and 885 nm increase (Fig. 6(b)). Well defined isosbestic points at 500, 730, and 942 nm and a light purple color ($x = 0.3236$ and $y = 0.3269$) were recorded after the second reduction reaction. Isosbestic points and color changes indicate formation of dianionic species form reduction of monoanionic ones. During the oxidation reaction while the bands at 624 and 680 nm decreases rapidly small bands are observed at 500 and 760 nm. Rapid decrease of the Q band and observation of new bands at LMCT regions illustrate Pc based oxidation and polymerization of the complex (Fig. 6(c)). Light yellow color ($x = 0.3435$ and $y = 0.3485$) was observed after the oxidation reaction as shown in Fig. 6(d).

CoPc gives different spectral changes than those of **H_2Pc**, **CuPc** and **NiPc** complexes, since redox activity of the metal center of CoPc. As shown in Fig. 7(a), the Q band of CoPc at 678 nm shift to 705 nm, while a new band at 468 nm is observed. Isosbestic point at 408, 552, and 753 nm indicate production of monoaninic reduced species. These spectral responses, especially shifting of the Q band indicate proceeding of $[Co^{II}Pc^{-2}]$ to $[Co^{I}Pc^{-2}]^{1-}$ during the R_1 redox reaction [48–50]. Light blue color ($x = 0.2908$ and $y = 0.3543$) of the complex changes to orange ($x = 0.3616$ and $y = 0.3855$) after the first reduction reaction. Fig. 7(b) represents the Pc based reduction of $[Co^{I}Pc^{-2}]^{1-}$ to $[Co^{I}Pc^{-3}]^{2-}$ during the R_2 redox reaction. While the Q band decreases, a new broad band is recorded at 540 nm, which are characteristic changes of Pc ring reduction

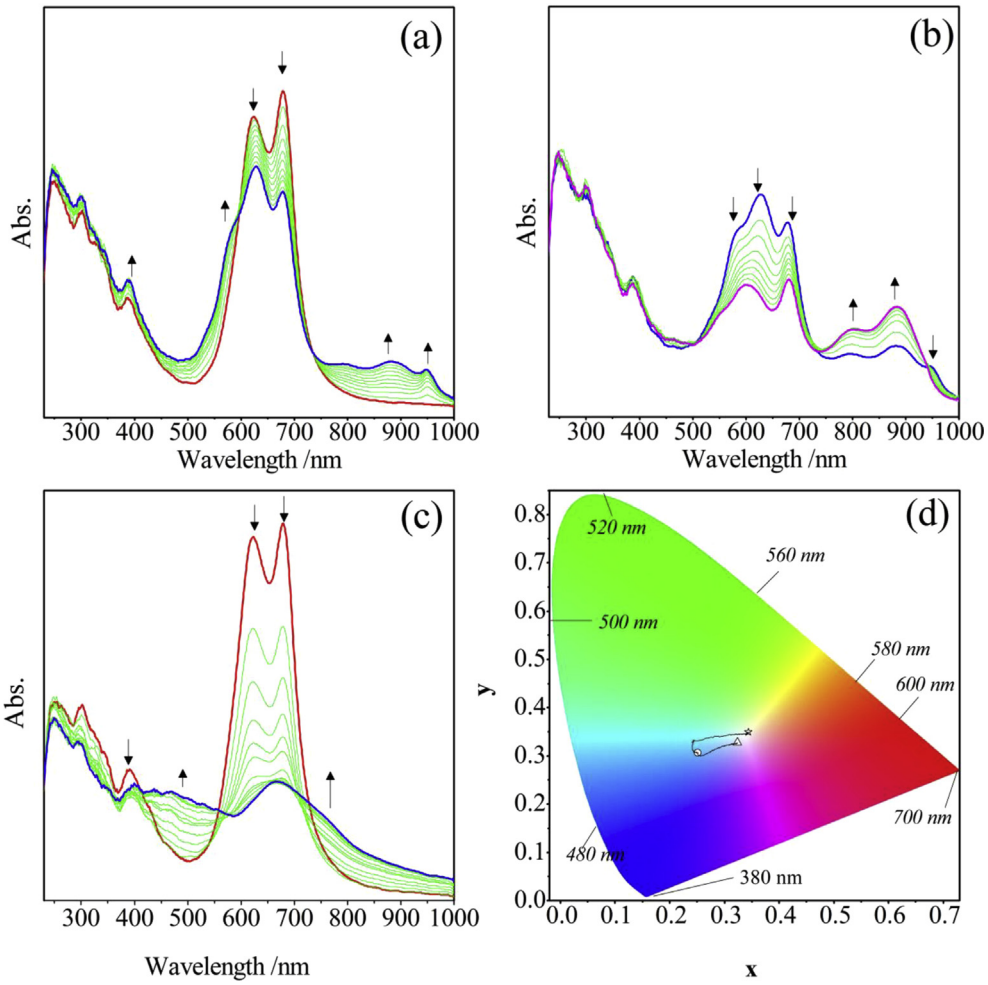

Fig. 6. In-situ UV–Vis spectral changes of **CuPc** ($1.0\ 10^{-4}$ mol dm^{-3}) in DCM/TBAP. a) $E_{app} = -0.50$ V b) $E_{app} = -1.50$ V c) $E_{app} = 1.50$ V d) Chromaticity diagram (each symbol represents the color of electro-generated species; : $[Cu^{II}Pc^{-2}]$, :$[Cu^{II}Pc^{-3}]^{-1}$ Δ: $[Cu^{II}Pc^{-4}]^{-2}$, ☆: polymer.

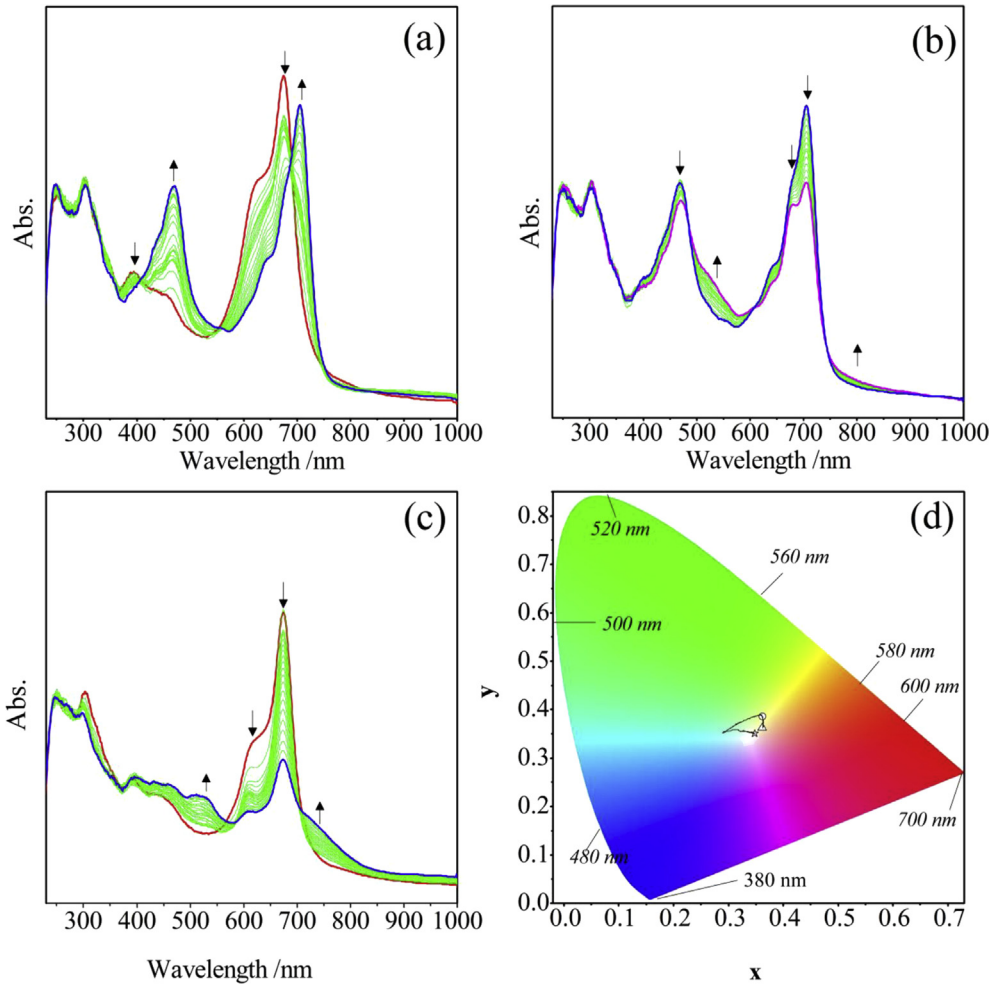

Fig. 7. In-situ UV–Vis spectral changes of **CoPc** (1.0 10^{-4} mol dm^{-3}) in DCM/TBAP. a) $E_{app} = -0.50$ V b) $E_{app} = -1.50$ V c) $E_{app} = 1.50$ V d) Chromaticity diagram (each symbol represents the color of electro-generated species; : $[Co^{II}Pc^{-2}]$, :$[Co^{I}Pc^{-2}]^{-1}$ Δ: $[Co^{I}Pc^{-3}]^{-2}$, ☆: polymer.

reactions. Isosbestic points at 487 and 743 nm support formation of $[Co^{I}Pc^{-3}]^{2-}$ species. Orange color ($x = 0.3622$ and $y = 0.3618$) is obtained after the second reduction reaction as shown in Fig. 7(d). Fig. 7(c) shows the spectral changes recorded during the oxidation reaction of CoPc. Decreasing of the Q band and observation of new bands at 530 and 745 nm are characteristic changes of the Pc oxidation reaction of CoPc during the R_1 redox reaction. Light orange color is recorded for the cationic species of CoPc obtained after the oxidation reaction. ($x = 0.3484$ and $y = 0.3506$).

Conclusion

In this study, the synthesis, spectral and electrochemical properties of soluble peripheral substituted metal-free, nickel(II), cobalt(II) and copper(II) phthalocyanines (**4**, **5**, **6** and **7**) are discussed. The target symmetrical phthalocyanines were separated by column chromatography which is placed aluminium oxide. All compounds were characterized by a combination of IR, ^{1}H NMR, ^{13}C NMR, UV–Vis and MS spectral data. Well defined reversible reduction reactions support the proposed structure of the complexes. Electropolymerization of the complexes also indicates presence of alkyl amino groups on the substituents of the complexes. All complex were electropolymerized on the working electrode and polymerization process of the complexes changes with altering of the metal center of the complexes. Formation of thin films with electropolymerization makes the complex as valuable functional materials for the preparation of various electrochemical devices, such as, electrocatalytic, electrochromic and electrosensing applications.

Acknowledgments

This study was supported by the Research Fund of Karadeniz Technical University, (project no: 8660) and The Scientific & Technological Research Council of Turkey (TÜBİTAK, project no: 111T963).

Appendix A. Supplementary data

Supplementary data related to this article can be found at http://dx.doi.org/10.1016/j.jorganchem.2014.06.006.

References

[1] K. Ishii, Coord. Chem. Rev. 256 (2012) 1556–1568.
[2] P. Kluson, M. Drobek, A. Kalaji, S. Zarubova, J. Krysa, J. Rakusan, J. Photochem. Photobiol. A Chem. 199 (2008) 267–273.
[3] G. Guillaud, J. Simon, J.P. Germain, Coord. Chem. Rev. 178 (1998) 1433–1484.
[4] K.R. Venugopala Reddy, J. Keshavayya, B.E. Kumara Swamy, M.N.K. Harish, H.R. Mallikarjuna, B.S. Sherigara, Dyes Pigm. 80 (2009) 1–5.
[5] F. Cicoira, N. Coppede, S. Iannotta, R. Martel, Appl. Phys. Lett. 98 (2011) 183303–183305.
[6] B. Meunier, Chem. Rev. 92 (1992) 1411–1456.
[7] N. Sehlotho, T. Nyokong, J. Mol. Catal. A Chem. 219 (2004) 201–207.

[8] M. Özer, F. Yilmaz, H. Erer, i. Kani, Ö. Bekaroğlu, Appl. Organomet. Chem. 23 (2009) 55–61.
[9] F. Yılmaz, M. Özer, İ. Kani, Ö. Bekaroğlu, Catal. Lett. 130 (2009) 642–647.
[10] J. Simon, C. Sirlin, Pure Appl. Chem. 6 (1989) 1625–1629.
[11] M. Durmuş, T. Nyokong, Inorg. Chem. Commun. 10 (2007) 332–338.
[12] Z. Bıyıklıoğlu, H. Kantekin, Synth. Met. 161 (2011) 943–948.
[13] S. Ünlü, M.N. Yaraşır, M. Kandaz, A. Koca, B. Salih, Polyhedron 27 (2008) 2805–2810.
[14] M.S. Ağırtaş, Dyes Pigm. 79 (2008) 247–251.
[15] B. Akkurt, E. Hamuryudan, Dyes Pigm. 79 (2008) 153–158.
[16] J. Sleven, C. Görller-Walrand, K. Binnemans, Mater. Sci. Engine. C 18 (2001) 229–238.
[17] İ. Yilmaz, A. Gürek, V. Ahsen, Polyhedron 24 (2005) 791–798.
[18] S.W. Oliver, T.D. Smith, Heterocyc 22 (1984) 2047–2052.
[19] R. Wang, W. Liu, Y. Chen, J.L. Zuo, X.Z. You, Dyes Pigm. 81 (2009) 40–44.
[20] A. Koca, Electrochem. Commun. 11 (2009) 838–841.
[21] M. Çamur, A.A. Esenpınar, A.R. Özkaya, M. Bulut, J. Organomet. Chem. 696 (2011) 1868–1873.
[22] E. Yabas, M. Sülü, S. Saydam, F. Dumludağ, B. Salih, Ö. Bekaroğlu, Inorg. Chim. Acta 365 (2011) 340–348.
[23] K.M. Kadish, T. Nakanishi, A.G. Gürek, V. Ahsen, İ. Yılmaz, J. Phys. Chem. 105 (2001) 9817–9821.
[24] İ. Yılmaz, T. Nakanishi, A.G. Gürek, K.M. Kadish, J. Porp. Phthalocyan. 7 (2003) 227–238.
[25] İ. Yılmaz, M. Koçak, Polyhedron 23 (2004) 1279–1285.
[26] Z. Bıyıklıoğlu, Dyes Pigm. 99 (2013) 59–66.
[27] J.G. Young, W. Onyebuagu, J. Org. Chem. 55 (1990) 2155–2159.
[28] Z. Bıyıklıoğlu, J. Organomet. Chem. 752 (2014) 59–66.
[29] D.D. Perrin, W.L.F. Armarego, Purification of Laboratory Chemicals, second ed., Pergamon Press, Oxford, 1989.
[30] C.F. van Nostrum, S.J. Picken, A.J. Schouten, R.J.M. Nolte, J. Am. Chem. Soc. 117 (1995) 9957–9965.
[31] T. Nyokong, Struct. Bond 135 (2010) 45–88.
[32] Z. Bıyıklıoğlu, İ. Acar, Synth. Met. 162 (2012) 1156–1163.
[33] M. Özer, A. Altındal, A.R. Özkaya, M. Bulut, Ö. Bekaroğlu, Polyhedron 25 (2006) 3593–3602.
[34] A. Atsay, A. Koca, M.B. Kocak, Transit. Met. Chem. 34 (2009) 877–890.
[35] N. Kobayashi, C.C. Leznoff, J. Porphyr. Phthalocyan. 8 (2004) 1015–1019.
[36] M.J. Trahan, Q.Y. Jia, S. Mukerjee, E.J. Plichta, M.A. Hendrickson, K.M. Abraham, J. Electrochem. Soc. 160 (2013) 1577–1586.
[37] A. Koca, A. Kalkan, Z.A. Bayir, Electrochim. Acta 56 (2011) 5513–5525.
[38] L. Cui, L.J. Chen, M.R. Xu, H.C. Su, S.Y. Ai, Anal. Chim. Acta 712 (2012) 64–71.
[39] P. Kissinger, W. R. H, Laboratory Techniques in Electroanalytical Chemistry, 2 ed., Marcel Decker, New York, 1996.
[40] E. Sürücü, G. Bolat, S. Abacı, J. Electroanal. Chem. 701 (2013) 20–24.
[41] G. Miluarek, Thin Sol. Films 517 (2009) 6100–6104.
[42] G. Muthuramana, Y.B. Shimb, J.H. Yoona, M.S. Won, Synth. Met. 150 (2005) 165–173.
[43] Z. Bıyıklıoğlu, D. Çakır, Dyes Pigm. 100 (2014) 150–157.
[44] H.R.P. Karaoğlu, A. Koca, M.B. Koçak, Synth. Met. 182 (2013) 1–8.
[45] İ. Özçeşmeci, A.K. Burat, Y. İpek, A. Koca, Z.A. Bayir, Electrochim. Acta 89 (2013) 270–277.
[46] H.T. Akçay, R. Bayrak, Ü. Demirbaş, A. Koca, H. Kantekin, İ. Değirmencioğlu, Dyes Pigm. 96 (2013) 483–494.
[47] I.A. Akinbulu, T. Nyokong, Polyhedron 29 (2010) 1257–1270.
[48] B. Agboola, K.I. Ozoemena, T. Nyokong, Electrochim. Acta 51 (2006) 4379.
[49] Y.H. Tse, A. Goel, M. Hu, C.C. Leznoff, J.E. Van Lier, A.B.P. Lever, Can. J. Chem. 71 (1993) 742–753.
[50] P. Matlaba, T. Nyokong, Polyhedron 21 (2002) 2463–2472.